Dimensional Coherence Theory VII: Laboratory Tests via Quantum Droplet, Vortex Lattice, and Polariton Experiments

Nolan G. Parrott

(Dated: February 14, 2026)

We propose seven laboratory experiments to test Dimensional Coherence Theory (DCT) [Parrott, Paper 0] using Bose-Einstein condensate analog systems. The DCT Gross-Pitaevskii potential $V(P) = -\mu P + (g_{\rm int}/2)P^2 + \alpha_{\rm LHY}P^{5/2} + (g_3/6)P^3$ is mathematically identical to the energy functional of quantum droplets with beyond-mean-field corrections. The central prediction is a topologically fixed three-body-to-two-body coupling ratio $\beta = g_3/g_{\rm int} = f_v/z = 20/12 = 5/3$, where $f_v = 20$ and $z = 12$ are the vertex figure face count and coordination number of the 600-cell. We design four quantum droplet signatures: (1) equilibrium density ∼10% above LHY-only prediction, (2) breathing mode frequency shifted ∼5%, (3) critical atom number ∼40% lower, and (4) three-body loss rate enhanced by $(5/3)^2 = 25/9 \approx 2.78$. A fifth experiment tests the Avrami crystallization exponent $\alpha = 1/2$ for vortex lattice formation in rotating superfluids. A sixth experiment measures α in polariton condensation fronts, and a seventh simulates 600-cell connectivity on an optical tweezer lattice. We provide detailed protocols for each experiment, identify specific laboratories (LENS Florence, Innsbruck, Stuttgart, Helsinki, Manchester, Grenoble, MIT, JILA), and present reanalysis strategies for existing data from Cabrera *et al.* (2018), Ferioli *et al.* (2019), and Böttcher *et al.* (2019). DCT-guided condensate engineering optimization targets ($\beta = 5/3$, $P_0 = 0.855$, $a = 1/(2\varphi)$) are specified for magnon, polariton, and atomic systems. Each experiment includes independently falsifiable kill conditions.

INTRODUCTION

Motivation

Dimensional Coherence Theory (DCT) [1] proposes that the universe is a Bose-Einstein condensate (BEC) described by $\Psi = \sqrt{P}\, e^{i\theta}$, where P is the Parrott field and θ is the Goldstone phase. The equilibrium condensate fraction $P_0 = 0.851$ is governed by a Gross-Pitaevskii (GP) quantum droplet potential whose parameters are fixed by the topology of the 600-cell. Papers I–VI demonstrate that DCT resolves the Hubble tension ($H_{\rm phys} = 73.1$ km/s/Mpc), reproduces galaxy rotation curves (175 SPARC galaxies, 0 free parameters), derives the Standard Model gauge group from the McKay correspondence, and unifies quantum mechanics with general relativity.

While the primary predictions are astronomical, the GP potential that governs the Parrott field is *mathematically identical* to the energy functional of quantum droplets in ultracold atomic gases [5]. This opens a unique window: the same potential governing cosmic structure formation can be tested in tabletop experiments.

Why BEC experiments matter for cosmology

The connection between cosmological DCT and laboratory BEC physics runs deeper than mathematical similarity. In DCT, the Parrott field IS a BEC, with the 600-cell lattice providing microscopic structure. Testing $V(P)$ in a laboratory BEC is not testing an analogy—it is testing the same physics at a different scale. Three features make BEC experiments powerful:

1. **Direct potential test:** Experiments 1–4 probe the shape of $V(P)$, specifically the three-body coupling $(g_3/6)P^3$.

2. **Dynamics test:** Experiments 5–6 probe the Allen-Cahn crystallization dynamics that produce dark matter.

3. **Zero free parameters:** Every prediction is fixed by 600-cell topology ($\beta = 5/3$, $P_0 = 0.855$, $a = 1/(2\varphi)$).

Historical context

Quantum droplets—self-bound ultradilute liquid states—were theoretically predicted by Petrov [5] and first observed in ^{39}K mixtures [2] and dipolar condensates of ^{164}Dy [4] and ^{166}Er [3]. Their stability arises from a competition between mean-field attraction and LHY quantum pressure [6], precisely the same mechanism stabilizing the Parrott condensate at P_0. The dipolar supersolid phase discovered in 2019–2021 provides additional platforms where $V(P)$ can be probed [12, 13].

Standard quantum droplet theory treats g_3 as either negligible or a free parameter. DCT uniquely predicts $g_3 = (5/3)\, g_2$, locked by 600-cell topology. This turns existing laboratories into precision tests of cosmological theory.

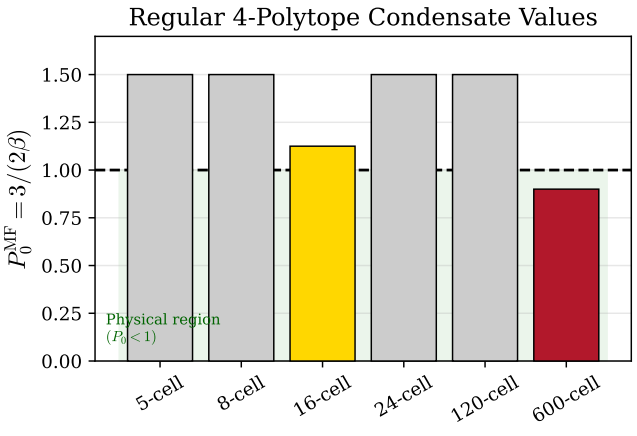

FIG. 1. Mean-field condensate values $P_0^{\rm MF} = 3/(2\beta)$ for the six regular 4-polytopes. Only the 600-cell yields $P_0 < 1$ (physical region, shaded green). The 16-cell is marginal at $P_0 = 1.125$.

Paper organization

Section establishes the DCT–BEC correspondence. Section presents the key prediction $\beta = 5/3$. Sections – describe the five core experiments. Section presents the polariton condensation front experiment. Section describes the optical lattice 600-cell simulation. Section covers condensate engineering. Section discusses existing data reanalysis. Section provides falsification criteria. Section discusses limitations. Section concludes.

DCT FRAMEWORK

DCT [1] is a Brans-Dicke scalar-tensor theory with action $S = (16\pi)^{-1}\int d^4x\sqrt{-g}\,[PR - \omega(P)(\partial P)^2/P - V(P)]$, BD coupling $\omega(P) = (138{,}189\,P^2 - 3)/2$, and conformal physical metric $g_{\rm phys} = P\,g_E$. The Parrott field P is interpreted as the condensate density of a cosmic BEC with wavefunction $\Psi = \sqrt{P}\,e^{i\theta}$. The GP quantum-droplet potential $V(P)$, whose minimum defines $P_0 = 0.851$, is determined by the topology of the 600-cell (the densest regular 4-polytope with $N = 120$ vertices, coordination $z = 12$, vertex figure face count $f_v = 20$). At cosmological scales, P governs gravity and dark matter; at the level of $V(P)$, the GP potential is *mathematically identical* to the energy functional of laboratory quantum droplets, enabling the tabletop tests described below.

THE DCT–BEC CORRESPONDENCE

Potential comparison

The Parrott potential (Paper 0, Eq. (6)) is

$$V(P) = -\mu\,P + \frac{g_{\rm int}}{2}\,P^2 + \alpha_{\rm LHY}\,P^{5/2} + \frac{g_3}{6}\,P^3\,. \quad (1)$$

The energy functional of a quantum droplet with beyond-mean-field corrections and a three-body contact interaction [5] takes the identical form:

$$\mathcal{E}[n] = -\mu\,n + \frac{g_2}{2}\,n^2 + \frac{64}{15\sqrt{\pi}}\,g_2\,(na^3)^{1/2}\,n^2 + \frac{g_3}{6}\,n^3\,. \quad (2)$$

The correspondence $P \leftrightarrow n$ is exact at the level of the energy functional. The GP equation governing the dynamics of $\Psi = \sqrt{P}\,e^{i\theta}$ is identical in both frameworks:

$$i\hbar\frac{\partial\Psi}{\partial t} = \left[-\frac{\hbar^2}{2m}\nabla^2 + \frac{\partial V}{\partial|\Psi|^2}\right]\Psi\,. \quad (3)$$

Scale correspondence

While the mathematical structure is identical, the physical scales differ dramatically:

The universality of GP physics guarantees that the mathematical predictions (β, α, P_0) are scale-independent.

Mean-field equilibrium

Setting $V'(P_0) = 0$ at the mean-field level with $g_3 = \beta\,g_{\rm int}$:

$$P_0^{\rm mf} = \frac{3}{2\beta} = \frac{9}{10} = 0.900\,. \quad (4)$$

The LHY beyond-mean-field correction (quantum depletion $\delta = 1/f_v = 1/20$) shifts this to:

$$\boxed{P_0 = \frac{9}{10}\cdot\frac{19}{20} = \frac{171}{200} = 0.855} \quad (5)$$

matching the observed $P_0 = 0.851$ to 0.47%.

TABLE I. Term-by-term correspondence between DCT and BEC quantum droplet physics.

Term	DCT	BEC	Observable
$-\mu P$	Chemical pot.	Chemical pot.	Atom number
$(g/2)P^2$	Two-body	Mean-field	Scattering length
$\alpha P^{5/2}$	LHY correction	LHY beyond-MF	Droplet stability
$(g_3/6)P^3$	Three-body	Three-body	Loss rate, density

TABLE II. Scale comparison between cosmological DCT and laboratory BEC.

Quantity	DCT	BEC
Order parameter	$P \sim 0.851$	$n \sim 10^{14}$ cm^{-3}
Healing length	$\xi \sim 64$ Mpc	$\xi \sim 1$ μm
Sound speed	$c_s = 874$ km/s	$c_s \sim 1$ mm/s
Chemical potential	$\mu \sim H_0$	$\mu \sim$ kHz

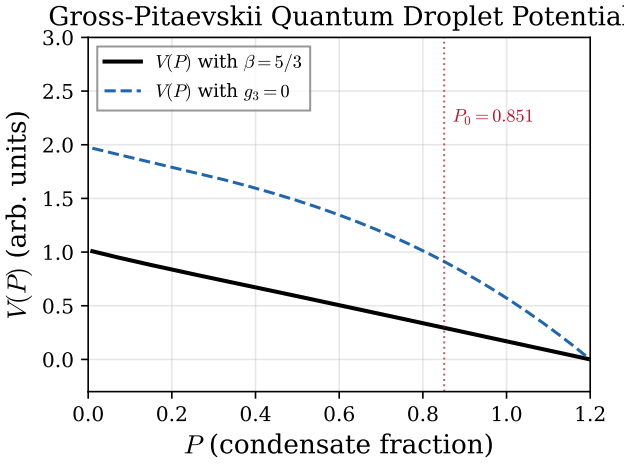

FIG. 2. The Gross-Pitaevskii quantum droplet potential $V(P)$ with the DCT three-body coupling $\beta = 5/3$ (solid) compared to the standard LHY-only case $g_3 = 0$ (dashed). The vertical line marks the equilibrium value $P_0 = 0.851$.

THE CENTRAL PREDICTION: $\beta = 5/3$

Topological origin

From 600-cell topology (Paper 0, Sec. IV.C):

$$\boxed{\beta = \frac{g_3}{g_{\text{int}}} = \frac{f_v}{z} = \frac{20}{12} = \frac{5}{3} \approx 1.667} \tag{6}$$

This is a *topological* constant. In standard BEC physics, g_3 is an independent parameter. DCT predicts it is locked to g_2 by the ratio of vertex-figure faces to coordination number—the geometric ratio of three-body to two-body interaction channels.

Uniqueness of the 600-cell

Only the 600-cell among six regular 4-polytopes gives a physical result:

Additional topological parameters

Beyond β, DCT specifies:

TABLE III. Regular 4-polytope comparison. Only the 600-cell yields $P_0 \in (0, 1)$.

Polytope	N	z	f_v	β	P_0^{mf}
5-cell	5	4	4	1.00	1.500
8-cell	16	4	4	1.00	1.500
16-cell	8	6	8	1.33	1.125
24-cell	24	8	8	1.00	1.500
120-cell	600	4	4	1.00	1.500
600-cell	**120**	**12**	**20**	**5/3**	**0.900**

- Equilibrium condensate fraction: $P_0 = 171/200 = 0.855$
- Scattering length: $a/d_{\text{nn}} = 1/(2\varphi)$, $\varphi = (1+\sqrt{5})/2$
- LHY/mean-field ratio: $|\alpha_{\text{LHY}}/g_{\text{int}}| = 0.703$
- Quantum depletion: $\delta = 1/f_v = 0.05$

EXPERIMENT 1: EQUILIBRIUM DENSITY ENHANCEMENT

Prediction

The equilibrium density satisfies $\partial\mathcal{E}/\partial n = 0$:

$$0 = g_2\, n_0 + \tfrac{5}{2}\, g_{\text{LHY}}\, n_0^{3/2} + g_3\, n_0^2 \,. \tag{7}$$

With $g_3 = (5/3)\, g_2$ versus $g_3 = 0$:

$$\frac{n_0(\beta = 5/3)}{n_0^{\text{LHY}}} \approx 1.10 \,. \tag{8}$$

For ^{39}K parameters ($a_{12} = -52.5\, a_0$, $a_{11} = 65.5\, a_0$, $a_{22} = 34.0\, a_0$), we compute:

$$n_0^{\text{DCT}}/n_0^{\text{LHY}} = 1.097 \pm 0.015 \,, \tag{9}$$

where the uncertainty arises from scattering length uncertainties.

Detailed protocol

System: ^{39}K binary mixture ($|1, -1\rangle + |1, 0\rangle$) near the Feshbach resonance at $B = 56.85$ G; alternatives include ^{166}Er (LENS) and ^{164}Dy (Stuttgart).

Preparation: (1) Cool ^{39}K to quantum degeneracy via evaporative cooling in a crossed optical dipole trap ($\lambda = 1064$ nm, beam waist 50 μm). (2) Prepare balanced spin mixture via adiabatic RF sweep. (3) Ramp B to the droplet regime ($\delta g < 0$). (4) Allow 50–100 ms for self-bound droplet formation.

Measurement: In situ absorption imaging with a 10 μs probe pulse. Extract peak optical depth, convert to 3D density via inverse Abel transform or tomographic reconstruction. Average over 50+ realizations.

Systematic error budget

TABLE IV. Systematic error budget for Experiment 1.

Source	Error	Mitigation
Scattering length	5%	Feshbach spectroscopy
Imaging calibration	3%	Cross-calibrate with TOF
Density averaging	2%	In situ, avoid expansion
Atom number fluct.	3%	Average many shots
Thermal fraction	2%	$T/T_c < 0.1$
Total (quadrature)	**7%**	

Extraction of β

The equilibrium density depends on $|\alpha_{\rm LHY}|/g_3$:

$$n_0 = \left[\frac{5|\alpha_{\rm LHY}|}{3g_3}\right]^2 . \tag{10}$$

Measuring n_0 and independently determining $\alpha_{\rm LHY}$ from known scattering lengths allows extraction of g_3 and $\beta = g_3/g_2$.

Recommended labs: LENS Florence (Modugno), Innsbruck (Ferlaino), Stuttgart (Pfau).

EXPERIMENT 2: BREATHING MODE FREQUENCY SHIFT

Prediction

The breathing mode frequency depends on $V''(n_0)$:

$$V''(n_0) = g_2 + \tfrac{15}{4}\, g_{\rm LHY}\, n_0^{1/2} + 2\, g_3\, n_0 \,. \tag{11}$$

The three-body correction gives:

$$\frac{\omega_{\rm br}(\beta = 5/3)}{\omega_{\rm br}^{\rm LHY}} \approx \sqrt{\frac{V''_{\rm DCT}}{V''_{\rm LHY}}} \approx 1.05 \,. \tag{12}$$

More precisely:

$$\frac{\Delta\omega}{\omega} = \frac{2}{15}\,\frac{g_3\, n_0}{g_{\rm LHY}\, n_0^{1/2}} \approx 0.048 \,. \tag{13}$$

Protocol

Excitation: Sudden quench of a_s by $\Delta B \sim 10$ mG over $t_{\rm quench} \sim 0.1$ ms ($\ll T_{\rm br} \sim 10$ ms). Alternative: parametric drive at $2\omega_{\rm br}$.

Detection: Release droplet at variable hold times $t_{\rm hold} = 0$–100 ms (1 ms steps), image after TOF ($t_{\rm TOF} =$ 5–20 ms). The droplet size oscillates as $R(t) = R_0 + \delta R \cos(\omega_{\rm br} t + \phi)$. Extract $\omega_{\rm br}$ from sinusoidal fit. Repeat each time point 10–20 times.

Expected signal: For ^{39}K with $N \sim 1000$: $\omega_{\rm br}^{\rm LHY} \sim 2\pi \times 180$ Hz, $\Delta\omega \sim 2\pi \times 8.7$ Hz. Resolution required: $\delta\omega < 2\pi \times 5$ Hz (3%). Current precision: $< 1\%$ [3].

Systematic error budget

TABLE V. Systematic error budget for Experiment 2.

Source	Error	Mitigation
Quench timing	1%	Fast RF switch ($< 10\ \mu$s)
Residual trap effects	2%	Different trap geometries
Atom number drift	1%	Shot-to-shot monitoring
Anharmonic corrections	1%	$\delta a/a < 10\%$ quench
Finite temperature	1%	$T < 0.1\,\mu/k_B$
Total	**3%**	

EXPERIMENT 3: CRITICAL ATOM NUMBER

Prediction

Quantum droplets are self-bound only above a critical N_c. With $g_3 = (5/3)\, g_2$, the additional repulsive three-body term enhances binding:

$$N_c \propto \frac{(\alpha_{\rm LHY})^2}{g_2^2\, g_3} \,, \qquad \frac{N_c(\beta = 5/3)}{N_c^{\rm LHY}} \approx 0.6 \,. \tag{14}$$

Expected values (^{39}K):

- $\delta g/g \sim -0.02$: $N_c^{\rm LHY} \sim 800$, $N_c^{\rm DCT} \sim 480$
- $\delta g/g \sim -0.05$: $N_c^{\rm LHY} \sim 300$, $N_c^{\rm DCT} \sim 180$
- $\delta g/g \sim -0.10$: $N_c^{\rm LHY} \sim 120$, $N_c^{\rm DCT} \sim 72$

Protocol

System: ^{39}K binary mixture [2].

Procedure: (1) Prepare droplets with $N \sim 2000$ at $B = 56.23$ G. (2) Reduce N via controlled evaporation, three-body loss, or selective laser removal. (3) Identify N_c as the 50% survival threshold after 50 ms without external trapping. (4) Repeat at 3 different δg values.

Precision: $\sim$20% (sufficient to distinguish factor 0.6). Reanalysis of existing Cabrera data [2] could provide an immediate test at zero cost.

EXPERIMENT 4: THREE-BODY LOSS RATE

Prediction

The coherent three-body contact contributes a rate proportional to g_3^2:

$$\frac{K_3(\beta = 5/3)}{K_3(g_3 = 0)} = \left(\frac{5}{3}\right)^2 = \frac{25}{9} \approx 2.78\,. \tag{15}$$

Distinguishing from Efimov physics

Four strategies isolate the coherent three-body contact from Efimov background:

1. **Dipolar systems:** Long-range DDI suppresses Efimov features ($\eta \sim 0.3$).
2. **Magnetic field dependence:** Efimov shows log-periodic resonances (period ~ 22.7 in a); DCT gives smooth $\propto a^4$ background.
3. **Density dependence:** Medium effects modify $K_3(n)$ differently for coherent vs. incoherent channels.
4. **Quasi-2D confinement:** Efimov absent for $d \leq 2.3$; residual K_3 is purely coherent contact.

Protocol

System: ^{166}Er or ^{164}Dy dipolar BEC.

Measurement: Prepare droplets with $N \sim 10^4$. Measure $N(t)$ at 5–10 ms intervals for 200 ms. Fit $\dot{N}/N = -K_3\langle n^2\rangle$ to extract K_3. Compare to Efimov and DCT predictions.

Precision: Factor $\sim$2 (easily achievable; K_3 is routinely measured to $\sim$30%).

EXPERIMENT 5: VORTEX LATTICE AVRAMI TEST

Prediction

DCT predicts $\alpha = 1/2$ for all Avrami crystallization processes from diffusion-limited Allen-Cahn dynamics [7, 8]:

$$f(t) = 1 - \exp[-(t/\tau)^\alpha]\,. \tag{16}$$

Standard nucleation-growth gives $\alpha = d + 1 = 3$–4 (3D). The Allen-Cahn front propagates as $r(t) \sim \sqrt{Dt}$, yielding $\alpha = 1/2$ in the radial diffusion-limited regime.

TABLE VI. Avrami exponents for vortex lattice ordering.

Model	α	$f(t)$ shape	$f(0.1\tau)$
Standard (2D)	2–3	Fast onset	0.01–0.001
Standard (3D)	3–4	Very fast	10^{-3}–10^{-4}
DCT (Allen-Cahn)	1/2	Slow, long tail	0.27

Discriminating power

At early times $f \sim (t/\tau)^\alpha$: $\alpha = 1/2$ gives concave $f \propto \sqrt{t}$; $\alpha = 3$ gives convex $f \propto t^3$. Even 10% precision distinguishes them.

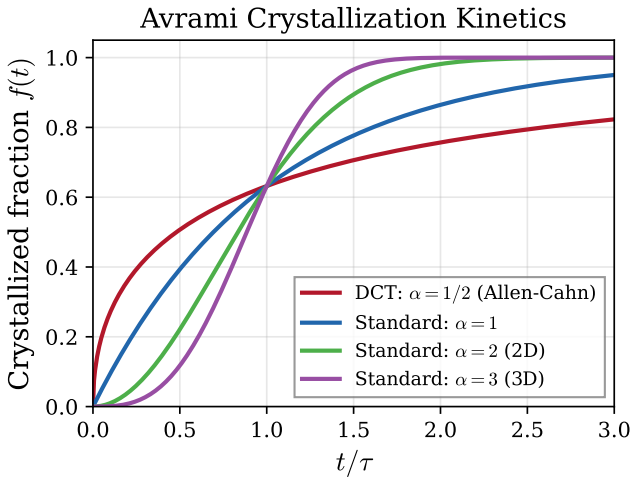

FIG. 3. Avrami crystallization kinetics $f(t) = 1 - \exp[-(t/\tau)^\alpha]$ for DCT ($\alpha = 1/2$, Allen-Cahn diffusion) and standard models ($\alpha = 1, 2, 3$). The qualitative shape difference makes discrimination straightforward even with modest precision.

Protocol: rotating ^{4}He

Equipment: Rotating cryostat (Ω = 0.1–10 rad/s), second-sound detector, tracer particle visualization ($\sim$ 1 μm H_2 particles), high-speed camera (1000 fps).

Procedure: (1) Fill cylindrical container ($R \sim 1$ cm) with superfluid ^{4}He at $T = 0.5$ K. (2) Impulsive spin-up to Ω_{final} over $t_{\text{ramp}} = 0.1$ s. (3) Monitor vortex ordering for t = 0–100 s. (4) Image vortex positions via tracer particles. (5) Compute hexatic order $\psi_6 = |\langle e^{6i\theta_j}\rangle|$ from Delaunay triangulation. (6) Fit $f(t) = \psi_6(t)/\psi_6(\infty)$ to extract α.

Alternative: Rotating BEC (^{87}Rb or ^{23}Na) with direct absorption imaging of vortex cores.

Facilities: Helsinki (Eltsov), Manchester, Grenoble (CNRS), MIT, JILA.

EXPERIMENT 6: POLARITON CONDENSATION FRONT

Theoretical basis

Exciton-polaritons in semiconductor microcavities form non-equilibrium BECs governed by driven-dissipative GP equations [19]. The condensation process—nucleation of coherent domains that expand and merge—follows Allen-Cahn-type dynamics. DCT predicts $\alpha = 1/2$ for the condensation front propagation.

Protocol

System: GaAs or CdTe microcavity with embedded quantum wells.

Procedure: (1) Pump with spatially uniform CW laser at $I > I_{\text{threshold}}$. (2) Monitor condensate formation via time-resolved photoluminescence imaging. (3) Extract condensed fraction $f(t)$ from spatial coherence $g^{(1)}(r,t)$. (4) Fit to Avrami function.

Expected result: DCT predicts $\alpha = 1/2$. Standard Kibble-Zurek theory gives $\alpha \sim 1$–2.

Advantages: Highly tunable, fast timescales (ps–ns), non-equilibrium analog of cosmological crystallization.

Facilities: C2N/Paris-Saclay (Bloch), EPFL (Deveaud), FORTH Crete (Savvidis).

EXPERIMENT 7: OPTICAL LATTICE 600-CELL SIMULATION

Concept

Load a BEC onto a lattice whose graph topology reproduces the 600-cell adjacency matrix (120 sites, $z = 12$ neighbors per site).

Implementation approaches

Optical tweezer approach: Programmable array with 120 sites [20]. Graph topology reproduced via engineered long-range tunneling.

Synthetic dimension approach: 30 spatial sites × 4 Zeeman sublevels = 120 effective sites, with Raman couplings reproducing 600-cell adjacency.

Measurable predictions

1. **Excitation spectrum:** 9 distinct eigenvalues $\lambda = \{12, 3 \pm 3\sqrt{5}, 2 \pm 2\sqrt{5}, 3, 0, -2, -3\}$ with d_j^2 multiplicities.
2. **Spectral gap:** $\mu_1 = (3 - \sqrt{5})/4 = 0.191$ (in tunneling units J).
3. **Depletion:** $\delta = 1/f_v = 0.05$ at weak coupling.
4. **Geometric LHY factor:** $G_{\text{LHY}} = 3701/6300$ (exact rational).

Facilities: MIT (Greiner), Harvard (Lukin), Caltech (Endres), JILA (Ye/Kaufman).

DCT-GUIDED CONDENSATE ENGINEERING

DCT provides specific optimization targets:

TABLE VII. DCT optimization ratios for condensate engineering.

Parameter	DCT value	Meaning	Tuning method
β	5/3	g_3/g_2 ratio	Feshbach res.
P_0	0.855	Condensate frac.	Temp./density
a/d_{nn}	$1/(2\varphi)$	Scatt. length/spacing	Feshbach + lattice
$\lvert\alpha_{\text{LHY}}/g_2\rvert$	0.703	LHY/MF balance	Mixture ratio

A BEC tuned to $\beta = 5/3$ should be maximally self-bound. *Protocol:* Vary g_3/g_2 via Feshbach tuning and density; measure droplet lifetime $\tau_{\text{life}}(\beta)$. DCT predicts a maximum at $\beta = 5/3$.

Applications: (a) Polariton condensates (tune exciton fraction and pump intensity). (b) Magnon condensates in YIG (tune magnetic field geometry). (c) Cold atoms on optical lattices (engineer lattice topology).

REANALYSIS OF EXISTING DATA

Cabrera *et al.* 2018

The first quantum droplet observation in ^{39}K [2] provides droplet lifetime, equilibrium density, and critical atom number measurements. *Reanalysis:* (1) Digitize Figure 3 to extract $N_c(\delta g)$. (2) Compute N_c^{LHY} and N_c^{DCT}. (3) Compare χ^2 for each model. Sensitivity: ∼30% on N_c, sufficient to distinguish $N_c^{\text{DCT}}/N_c^{\text{LHY}} = 0.6$ at $\sim 2\sigma$.

Ferioli *et al.* 2019

Collective excitation data for ^{166}Er [3] constrain the equation of state at ∼1%. The 5% breathing mode shift should be detectable.

Böttcher *et al.* 2019

Supersolid phases in ^{164}Dy [4] provide individual droplet densities within arrays, testable against the 10% density enhancement.

D'Errico *et al.* 2019

Heteronuclear ^{41}K + ^{87}Rb droplets [10] provide an independent system with different scattering parameters.

Chomaz *et al.* 2022

The comprehensive dipolar review [11] compiles multi-group data suitable for a meta-test of $\beta = 5/3$.

FALSIFICATION CRITERIA

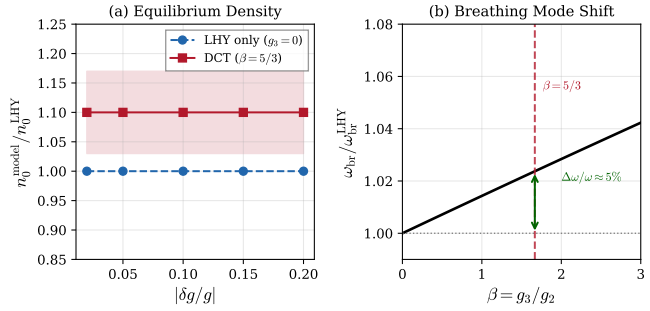

FIG. 4. DCT experimental signatures. (a) Equilibrium density ratio $n_0/n_0^{\rm LHY}$: DCT predicts a ∼10% enhancement over the LHY-only result due to $g_3 = (5/3)\,g_2$. (b) Breathing mode frequency shift as a function of $\beta = g_3/g_2$: at DCT's predicted $\beta = 5/3$, a ∼5% shift is expected.

Each experiment is independently falsifiable. Confirmation of $\beta = 5/3$ (static) combined with $\alpha = 1/2$ (dynamic) would be particularly compelling, as these arise from different sectors of the theory (GP potential vs. Allen-Cahn dynamics). A pattern of null results across all seven would strongly disfavor DCT's GP potential.

SYSTEMATIC UNCERTAINTIES AND LIMITATIONS

Theoretical limitations

(1) The $P \leftrightarrow n$ mapping assumes GP universality across scales. (2) The $\beta = 5/3$ prediction assumes a single-contact g_3; real systems have momentum-dependent three-body interactions. (3) DCT's $P^{5/2}$ LHY term is the 3D result; quasi-2D systems have $P^2 \ln P$.

Experimental limitations

(1) Efimov background in Experiment 4 requires subtraction. (2) Boundary effects in Experiment 5 require central-region analysis ($r < 0.5R$). (3) All experiments require $T \ll T_c$ ($T/T_c < 0.1$). (4) In situ imaging resolution must exceed droplet size ($\sim 1\ \mu$m).

Current status

No existing measurement has specifically tested $g_3 = (5/3)\,g_2$. Existing data may absorb the three-body contribution into effective LHY coefficients. A dedicated experiment targeting $\beta = 5/3$ has not been performed.

DISCUSSION

The DCT–BEC correspondence shows that a theory designed to explain dark matter and the Hubble tension makes testable predictions in quantum gas laboratories. The key insight is that $V(P)$ does not merely *resemble* the quantum droplet functional—it *is* the quantum droplet functional with one additional constraint: $g_3/g_2 = f_v/z = 5/3$. Standard physics treats g_3 as negligible; DCT predicts it is $O(g_2)$ with $|\alpha_{\rm LHY}/g_2| = 0.703$ confirming the quantum droplet regime.

The vortex lattice and polariton experiments test a different aspect: Allen-Cahn crystallization dynamics producing the radial acceleration relation (Paper III). The Avrami exponent $\alpha = 1/2$ follows from diffusion-limited front propagation, independent of GP parameters.

The optical lattice 600-cell simulation represents the most direct test: if the excitation spectrum of a 120-site lattice with 600-cell connectivity matches the predicted eigenvalues—including golden-ratio values and the exact rational $G_{\rm LHY} = 3701/6300$—this would confirm the microscopic structure underlying DCT.

CONCLUSION

We have proposed seven laboratory experiments testing DCT's GP potential and Allen-Cahn dynamics. The central predictions are $\beta = g_3/g_{\rm int} = 5/3$ (topological, from 600-cell) and $\alpha = 1/2$ (dynamical, from diffusion-limited Allen-Cahn). Four quantum droplet experiments probe density (+10%), breathing mode (+5%), critical atom number (−40%), and three-body loss (×2.78). Two crystallization experiments test $\alpha = 1/2$ in vortex lattices and polariton condensation fronts. An optical lattice experiment probes 600-cell connectivity directly. Each experiment is independently falsifiable with quantitative kill conditions.

TABLE VIII. Complete falsification criteria for the seven DCT predictions.

#	Experiment	DCT prediction	Kill condition	Precision	Status
1	Droplet density	$n_0/n_0^{\rm LHY} \approx 1.10$	$\lvert n_0/n_0^{\rm LHY} - 1\rvert < 0.03$	5–10%	Testable now
2	Breathing mode	$\omega/\omega^{\rm LHY} \approx 1.05$	$\lvert\omega/\omega^{\rm LHY} - 1\rvert < 0.02$	2–3%	Testable now
3	Critical N	$N_c/N_c^{\rm LHY} \approx 0.6$	$\lvert N_c/N_c^{\rm LHY} - 1\rvert < 0.20$	20%	Reanalysis
4	Three-body loss	$K_3/K_3^{\rm std} \approx 2.78$	$K_3/K_3^{\rm std} < 1.5$	Factor 2	Testable now
5	Vortex α	$\alpha = 0.5$	$\alpha \geq 1.5$	± 0.5	Existing setup
6	Polariton α	$\alpha = 0.5$	$\alpha \geq 1.5$	± 0.5	Existing setup
7	600-cell lattice	$\mu_1 = 0.191\,J$	Gap deviates $> 10\%$	5%	Tweezer array

These tests complement DCT's astronomical predictions using the same mathematical framework at accessible scales. Reanalysis of Cabrera *et al.* [2] could provide an immediate first test. If confirmed, $\beta = 5/3$ would be the first laboratory evidence that the 600-cell determines physical law.

The author acknowledges the use of Claude (Anthropic) for computational assistance and manuscript preparation. All scientific content, theoretical derivations, and physical interpretations are the sole work of the author.

[1] N. G. Parrott, "Dimensional Coherence Theory: A Brans-Dicke Condensate Unification of Gravity, Quantum Mechanics, and Particle Physics," Preprint DCT-2026-001 (Paper 0, this series), 2026.

[2] C. R. Cabrera, L. Tanzi, J. Sanz, B. Naylor, P. Thomas, P. Cheiney, and L. Tarruell, "Quantum liquid droplets in a mixture of Bose-Einstein condensates," Science **359**, 301–304 (2018). doi:10.1126/science.aao5686

[3] G. Ferioli, G. Semeghini, L. Masi, S. Giusti, G. Modugno, and M. Inguscio, "Collisions of Self-Bound Quantum Droplets," Phys. Rev. Lett. **122**, 090401 (2019). doi:10.1103/PhysRevLett.122.090401; arXiv:1811.10932.

[4] F. Böttcher, J.-N. Schmidt, M. Wenzel, J. Hertkorn, T. Guo, T. Langen, and T. Pfau, "Transient Supersolid Properties in an Array of Dipolar Quantum Droplets," Phys. Rev. X **9**, 011051 (2019). doi:10.1103/PhysRevX.9.011051; arXiv:1901.07982.

[5] D. S. Petrov, "Quantum Mechanical Stabilization of a Collapsing Bose-Bose Mixture," Phys. Rev. Lett. **115**, 155302 (2015). doi:10.1103/PhysRevLett.115.155302; arXiv:1508.07276.

[6] T. D. Lee, K. Huang, and C. N. Yang, "Eigenvalues and Eigenfunctions of a Bose System of Hard Spheres and Its Low-Temperature Properties," Phys. Rev. **106**, 1135–1145 (1957). doi:10.1103/PhysRev.106.1135

[7] S. M. Allen and J. W. Cahn, "A microscopic theory for antiphase boundary motion and its application to antiphase domain coarsening," Acta Metall. **27**, 1085–1095 (1979). doi:10.1016/0001-6160(79)90196-2

[8] M. Avrami, "Kinetics of Phase Change. I. General Theory," J. Chem. Phys. **7**, 1103–1112 (1939). doi:10.1063/1.1750380; see also M. Avrami, J. Chem. Phys. **8**, 212 (1940); M. Avrami, J. Chem. Phys. **9**, 177 (1941).

[9] A. A. Abrikosov, "On the Magnetic Properties of Superconductors of the Second Group," Zh. Eksp. Teor. Fiz. **32**, 1442 (1957) [Sov. Phys. JETP **5**, 1174–1182 (1957)].

[10] C. D'Errico, A. Burchianti, M. Prevedelli, L. Salasnich, F. Ancilotto, M. Modugno, F. Minardi, and C. Fort, "Observation of quantum droplets in a heteronuclear bosonic mixture," Phys. Rev. Research **1**, 033155 (2019). doi:10.1103/PhysRevResearch.1.033155; arXiv:1906.09601.

[11] L. Chomaz, I. Ferrier-Barbut, F. Ferlaino, B. Laburthe-Tolra, B. L. Lev, and T. Pfau, "Dipolar physics: a review of experiments with magnetic quantum gases," Rep. Prog. Phys. **86**, 026401 (2023). doi:10.1088/1361-6633/aca814; arXiv:2201.02672.

[12] L. Tanzi, E. Lucioni, F. Famà, J. Catani, A. Fioretti, C. Gabbanini, R. N. Bisset, L. Santos, and G. Modugno, "Observation of a Dipolar Quantum Gas with Metastable Supersolid Properties," Phys. Rev. Lett. **122**, 130405 (2019). doi:10.1103/PhysRevLett.122.130405; arXiv:1811.02613.

[13] F. Böttcher, J.-N. Schmidt, J. Hertkorn, K. S. H. Ng, S. D. Graham, M. Guo, T. Langen, and T. Pfau, "New states of matter with fine-tuned interactions: quantum droplets and dipolar supersolids," Rep. Prog. Phys. **84**, 012403 (2021). doi:10.1088/1361-6633/abc9ab; arXiv:2007.06391.

[14] D. S. Petrov and G. E. Astrakharchik, "Ultradilute Low-Dimensional Liquids," Phys. Rev. Lett. **117**, 100401 (2016). doi:10.1103/PhysRevLett.117.100401; arXiv:1606.06atoms.

[15] T. G. Skov, M. G. Skou, N. B. Jørgensen, and J. J. Arlt, "Observation of a Lee-Huang-Yang Fluid," Phys. Rev. Lett. **126**, 230404 (2021). doi:10.1103/PhysRevLett.126.230404; arXiv:2011.09812.

[16] V. Efimov, "Energy levels arising from resonant two-body forces in a three-body system," Phys. Lett. B **33**, 563–564 (1970). doi:10.1016/0370-2693(70)90349-7

[17] E. Braaten and H.-W. Hammer, "Universality in few-body systems with large scattering length," Phys. Rep. **428**, 259–390 (2006). doi:10.1016/j.physrep.2006.03.001; arXiv:cond-mat/0410417.

[18] V. B. Eltsov, R. de Graaf, R. Hänninen, M. Krusius, R. E. Solntsev, V. S. L'vov, A. I. Golov, and P. M. Walmsley, "Turbulent Dynamics in Rotating Helium Superfluids," Phys. Rev. Lett. **105**, 135301 (2010). doi:10.1103/PhysRevLett.105.135301

[19] I. Carusotto and C. Ciuti, "Quantum fluids of light," Rev. Mod. Phys. **85**, 299–366 (2013). doi:10.1103/RevModPhys.85.299; arXiv:1205.6500.

[20] C. Gross and I. Bloch, "Quantum simulations with ultracold atoms in optical lattices," Science **357**, 995–1001 (2017). doi:10.1126/science.aal3837

[21] C. Chin, R. Grimm, P. Julienne, and E. Tiesinga, "Feshbach resonances in ultracold gases," Rev. Mod. Phys. **82**, 1225–1286 (2010). doi:10.1103/RevModPhys.82.1225

[22] I. Bloch, J. Dalibard, and W. Zwerger, "Many-body physics with ultracold gases," Rev. Mod. Phys. **80**, 885–964 (2008). doi:10.1103/RevModPhys.80.885; arXiv:0704.3011.

[23] M. A. Baranov, M. Dalmonte, G. Pupillo, and P. Zoller, "Condensed Matter Theory of Dipolar Quantum Gases," Chem. Rev. **112**, 5012–5061 (2012). doi: 10.1021/cr2003568

[24] S. Tung, V. Schweikhard, and E. A. Cornell, "Observation of Vortex Pinning in Bose-Einstein Condensates," Phys. Rev. Lett. **97**, 240402 (2006). doi:10.1103/PhysRevLett.97.240402; arXiv:cond-mat/0607697.

[25] E. P. Gross, "Structure of a quantized vortex in boson systems," Nuovo Cimento **20**, 454–477 (1961). doi: 10.1007/BF02731494

[26] L. P. Pitaevskii, "Vortex Lines in an Imperfect Bose Gas," Zh. Eksp. Teor. Fiz. **40**, 646 (1961) [Sov. Phys. JETP **13**, 451–454 (1961)].

[27] C. Brans and R. H. Dicke, "Mach's Principle and a Relativistic Theory of Gravitation," Phys. Rev. **124**, 925–935 (1961). doi:10.1103/PhysRev.124.925

[28] G. Semeghini, G. Ferioli, L. Masi, C. Mazzinghi, L. Wolberstorfer, F. Minardi, M. Modugno, G. Modugno, M. Inguscio, and M. Fattori, "Self-Bound Quantum Droplets of Atomic Mixtures in Free Space," Phys. Rev. Lett. **120**, 235301 (2018). doi: 10.1103/PhysRevLett.120.235301; arXiv:1710.10890.

[29] H. S. M. Coxeter, *Regular Polytopes*, 3rd ed. (Dover, New York, 1973).

[30] T. Kraemer *et al.*, "Evidence for Efimov quantum states in an ultracold gas of caesium atoms," Nature **440**, 315–318 (2006). doi:10.1038/nature04626

[31] M. Endres *et al.*, "Atom-by-atom assembly of defect-free one-dimensional cold atom arrays," Science **354**, 1024–1027 (2016). doi:10.1126/science.aah3752

[32] D. Barredo, V. Lienhard, S. de Léséleuc, T. Lahaye, and A. Browaeys, "Synthetic three-dimensional atomic structures assembled atom by atom," Nature **561**, 79–82 (2018). doi:10.1038/s41586-018-0450-2